NeuroImage 60 (2012) 2323–2334

Contents lists available at SciVerse ScienceDirect

NeuroImage

journal homepage: www.elsevier.com/locate/ynimg

Meanfield modeling of propofol-induced changes in spontaneous EEG rhythms

Rikkert Hindriks [a,*], Michel J.A.M. van Putten [a,b]

[a] Department of Clinical Neurophysiology, MIRA-Institute for Biomedical Technology and Technical Medicine, University of Twente, 7500 AE Enschede, The Netherlands
[b] Department of Neurology and Clinical Neurophysiology, Medisch Spectrum Twente, Enschede, The Netherlands

ARTICLE INFO

Article history:
Accepted 16 February 2012
Available online 28 February 2012

Keywords:
EEG
Anesthesia
Propofol
Meanfield

ABSTRACT

During the maintenance period of propofol-induced general anesthesia, specific changes in spontaneous EEG rhythms can be observed. These comprise increased delta and theta power and the emergence of alpha oscillations over frontal regions. In this study we use a meanfield model of the thalamo-cortical system to reproduce these changes and to elucidate the underlying mechanisms. The model is able to reproduce the most dominant changes in the EEG and suggests that they are caused by the amplification of resonances within the thalamo-cortical system. Specifically, while observed increases in delta and alpha power are reflections of amplified resonances in the respective frequency bands, increases in theta power are caused indirectly by spectral power leakage from delta and alpha bands. The model suggests that these changes are brought about through increased inhibition within local cortical interneuron circuits. These results are encouraging and motivate more extensive use of neural meanfield models in elucidating the physiological mechanisms underlying the effects of pharmacological agents on macroscopic brain dynamics.

Introduction

The accomplishments of today's surgical procedures are unthinkable without the use of anesthetic agents, with their power to produce sedation, unconsciousness, and complete amnesia. While the molecular and cellular mechanisms underlying the actions of general anesthetics are gradually being revealed (Hemmings et al., 2005; Rudolph and Antkowiak, 2004) the way in which they affect global brain functioning—thereby causing unconsciousness and amnesia—are still poorly understood (Brown et al., 2010). The biophysical correlates of anesthetic-induced changes in global brain functioning can be investigated by the use of electroencephalography (EEG), positon emission tomography (PET), and functional magnetic resonance imaging (fMRI). Therefore, elucidation of the biophysical mechanisms underlying anesthetic-induced changes in the signals obtained through these imaging modalities provides an essential step in mapping the neural correlates of consciousness and amnesia. Of special importance in this context is the EEG, as it provides direct measurements of electrophysiological processes and displays dynamics on timescales similar as on which cognitive events take place.

The intravenous anesthetic agent propofol (2,6-di-isopropylphenol) elicits a range of dose-dependent EEG responses. During the induction phase, enhanced oscillatory activity within several frequency bands can be observed. This enhanced activity is suppressed for higher concentrations, giving way to an overall depression of EEG activity. These dose-dependent changes of oscillatory activity, with an initial increase at relatively low concentrations, and a subsequent decrease with increasing concentrations, are referred to as *bi-phasic responses* or *induction sequences* (Johnson et al., 2003; Kuizenga et al., 2001; San-juan et al., 2010). For increasingly deeper levels of general anesthesia one can observe alpha spindles (Huotari, 2004), burst-suppression patterns, sustained slow waves (Hazeaux et al., 1987), and even iso-electricity (Doyle and Matta, 1999; Lukatch et al., 2005). For propofol concentrations that are commonly used to perform surgical procedures with EEG monitoring, for instance during carotid endarterectomy (van Putten et al., 2004) the anesthesiologist aims to realize a continuous EEG pattern characterized by an enhancement of EEG power with pronounced alpha oscillations. Additional characteristics of the EEG at these concentrations of propofol include an increase in alpha peak-frequency, especially over frontal regions, accompanied by increases in delta and theta power (Feshchenko et al., 2004; Gugino et al., 2001; Hazeaux et al., 1987; San-juan et al., 2010; Schwender et al., 1996). In this study we provide an integrated explanation of the observed frontal alpha oscillations and increases in delta and theta power by adopting a meanfield approach to large-scale brain dynamics.

Meanfield models of neural activity are constructed by averaging microscopic variables like neuronal membrane potentials and firing rates over local pieces of neural tissue (Wilson and Cowan, 1973). This averaging enables linking cellular physiology to large-scale brain dynamics as reflected in the EEG, PET, and fMRI (Deco et al., 2008). Although neural meanfield models have a long tradition (Amari, 1977; Freeman, 2004; Lopes da Silva et al., 1974; Wilson and Cowan, 1973) and have been applied to a wide variety of EEG phenomena (Breakspear et al.,

* Corresponding author.
E-mail address: R.Hindriks@utwente.nl (R. Hindriks).

1053-8119/$ – see front matter © 2012 Elsevier Inc. All rights reserved.
doi:10.1016/j.neuroimage.2012.02.042

2006; Daunizeau et al., 2009; David et al., 2005; Jansen and Rit, 1995; Jirsa and Haken, 1996; Liley and Cadusch, 2002; Rennie et al., 2002; Robinson et al., 2001; Steyn-Ross et al., 2005) to name only a few, their application to anesthetic-induced EEG changes is relatively recent (Bojak and Liley, 2005; Foster et al., 2008; Hutt and Longtin, 2010; Liley and Bojak, 2005; Liley et al., 2003; Molaee-Ardekani et al., 2007; Steyn-Ross et al., 1999). While Molaee-Ardekani et al. (2007) focus on slow EEG oscillations observed during deeper levels of desflurane-induced general anesthesia and (Liley and Bojak, 2005) model the proconvulsive properties of several volatile anesthetic agents, most modeling efforts aim at understanding the dynamical mechanisms underlying bi-phasic responses (Bojak and Liley, 2005; Hutt and Longtin, 2010; Steyn-Ross et al., 1999). In this study, we concentrate on modeling the details of the first phase of the bi-phasic response induced by propofol which comprises pronounced alpha oscillations with increased peak-frequency, accompanied by increases in delta and theta power (Feshchenko et al., 2004; Gugino et al., 2001; Hazeaux et al., 1987; San-juan et al., 2010; Schwender et al., 1996). The existing studies modeling these phenomena are limited to Ching et al. (2010) in which a conductance-based network model is constructed that accounts for the enhancement of alpha oscillations. The simultaneous increase delta and theta power, however, was not demonstrated. Providing an integrated explanation for the enhancement of alpha oscillations and the simultaneous increases in delta and theta power is the main focus of this study.

The above mentioned meanfield studies are based on purely cortical theories of EEG generation (Hutt and Longtin, 2010; Liley and Cadusch, 2002). Ching et al. (2010) suggested the thalamus to play a key role in the generation of the propofol-induced alpha rhythm. In general, anesthetic agents do target subcortical structures (Rudolph and Antkowiak, 2004) and are known to alter their functional properties (Alkire et al., 1995; Fiset et al., 1999; Mhuircheartaigh et al., 2010; Velly et al., 2007; White and Alkire, 2003). Especially the thalamus, which is known to play a fundamental role in the regulation of attention and sleep (Brown et al., 2010; Kandel et al., 2000), is suggested to play a key role in anesthetic-induced changes in consciousness (Alkire et al., 2000, 2008). Our starting point for modeling therefore, will be a meanfield model of the cortex in which thalamic feedback is incorporated.

To elucidate the physiological mechanisms underlying the above described changes in EEG activity that can be observed during the maintenance period of propofol-induced general anesthesia, we use the meanfield model described in Rennie et al. (2002) and Robinson et al. (2001). In Section 2.1 we describe the EEG phenomenology using data recorded from subjects that underwent surgery for which propofol was used. In Section 2.2 we outline the basic thalamo-cortical meanfield model and in Section 2.3 we describe how to incorporate the action of propofol. In Section 2.4 we derive formulas for the cortical transfer function and theoretical EEG power spectrum, which we will use in subsequent sections. In Section 3.1 we demonstrate that the model reproduces the EEG phenomenology. In Sections 3.2 and 3.3 we describe the underlying dynamical mechanisms suggested by the model.

Materials and methods

EEG recordings and phenomenology

The data consists of EEG recordings of 17 patients that underwent surgery for carotid endarterectomy. In all these patients, the EEG was recorded as a standard procedure to determine if temporary shunting is needed (van Putten et al., 2004). The recordings were collected from the Neurocenter EEG database from the Medisch Spectrum Twente, Enschede, The Netherlands. Propofol was used both for the induction and maintenance of anesthesia, with dosages in the range of 200–300 mg/h. As part of the routine procedure, baseline EEG recordings are made 1 day before surgery including eyes-closed resting-state conditions. We refer to these conditions as *anesthesia* and *baseline*, respectively. The data selection consisted of single epochs of variable length (minimum 41 sec, maximum 210 sec) that were visually screened and selected based on the absence of artifacts. We selected those subjects whose EEG showed an increase in alpha power at electrode Fz relative to baseline. This resulted in the selection of 9 subjects (five males, average age 66.4, std 8.4 years and four females, average age 66.0, std 3.2 years). While alpha activity is commonly defined as activity between 8 and 13 Hz, in our data-set alpha peaks tend to be lower probably due to the selection of a frontal electrode and the relatively high age of the subjects. Therefore, in this study we understand alpha activity as rhythmic activity between 6 and 13 Hz. Moreover, delta and theta are defined as rhythmic activity between 0.5 and 3 and between 3 and 6 Hz, respectively. Throughout the analysis we used EEG time series recorded from electrode Fz using an average montage. The selected epochs were bandpass filtered between 0.5 and 40 Hz using a 4-th order zero-phase Butterworth filter. All routines were carried out in MATLAB.

Fig. 1 shows data of a single subject. Figs. 1(b) and (d) show ten-second EEG traces recorded from electrode Fz during baseline and under anesthesia, respectively. Fig. 1(a) displays the topographic distribution of power within the alpha band under anesthesia. As the figure illustrates, the propofol-induced alpha oscillations can be observed especially in frontal regions, in agreement with previous observations (Feshchenko et al., 2004; Gugino et al., 2001). Fig. 1(c) shows the corresponding EEG power spectra, illustrating increases in delta and theta power, as well as more pronounced alpha oscillations with increased peak-frequency relative to baseline. These changes are similar as those reported in Feshchenko et al. (2004), Gugino et al. (2001), Hazeaux et al. (1987), San-juan et al. (2010), Schwender et al. (1996).

Thalamo-cortical model

In this section we describe the neural meanfield model presented in Rennie et al. (2002). It models the dynamics of locally averaged membrane potentials of different neurons types within the thalamo-cortical system. Four different neuron types are distinguished: cortical pyramidal neurons, cortical inhibitory neurons, thalamic reticular neurons, and thalamo-cortical relay neurons. We denote these neural types by $a \in \{e, i, r, s\}$, where e, i, r, and s denote pyramidal, inhibitory, reticular, and relay neurons, respectively, The average soma membrane potential of neurons of type a is denoted by V_a. The average firing rate $Q_a = S(V_a)$ in Hz of neurons of type a is determined by V_a through the activation function S:

$$S(V_a) = \frac{Q_{\max}}{1 + exp(-(V_a - \theta)/\sigma)}, \tag{1}$$

where $Q_{\max}$ is the maximal firing rate in Hz, θ is the average activation threshold in mV, and σ is proportional to the standard deviation of activation thresholds over the neuronal population.

Incoming firing rates induce a transient perturbation of the average post-synaptic membrane potential, which is described by the synaptic response function

$$\bar{h}(t) = \frac{\alpha\beta}{\beta - \alpha}\left(e^{-\alpha t} - e^{-\beta t}\right), \tag{2}$$

where $\beta > \alpha$ and β and α denote the synaptic rise and decay rates in s^{-1}, respectively. The synaptic response $\bar{h}$ models the average response at the cell bodies thereby combining post-synaptic responses as well as delays within the dendritic trees (Robinson et al., 1997). The average firing rate $Q_e(x, t)$ of pyramidal neurons at position x on the cortical sheet and time t spread out through long-range fibers according to the wave equation

$$D\phi_e(x, t) = Q_e(x, t), \tag{3}$$

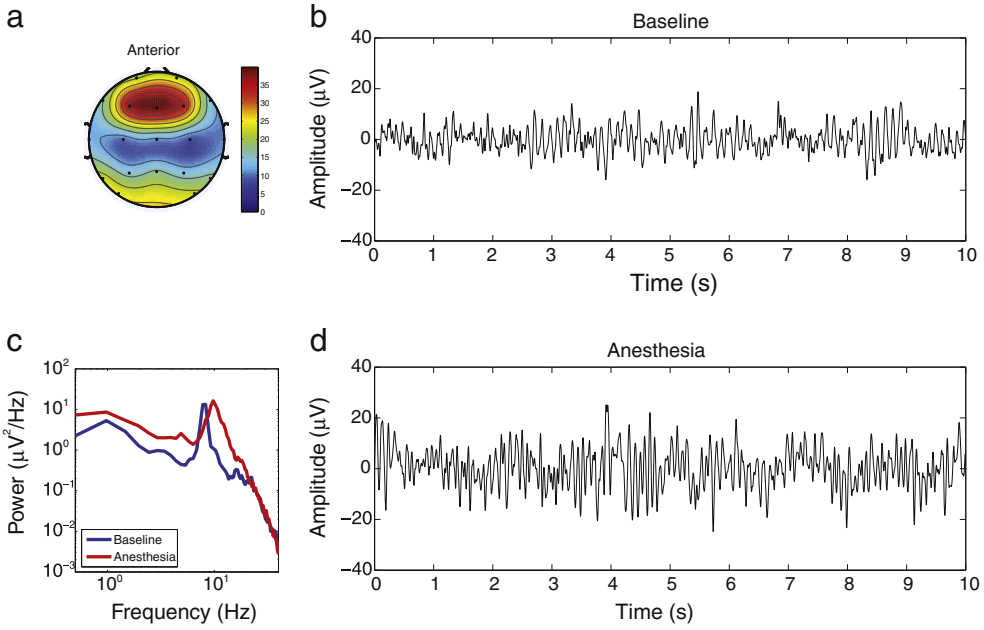

Fig. 1. Propofol-induced changes in spontaneous EEG activity. (a) Topography of EEG power within the alpha band (6–13 Hz) during the maintenance period of propofol-induced general anesthesia. (b) and (d) show EEG time-series from electrode Fz during wakefulness and propofol-induced general anesthesia, respectively. (c) EEG power spectrum derived from the time-series in (b) and (c). All figures are based on EEG data from a single representative subject.

where D denotes the wave operator

$$D = \left(\frac{1}{\gamma}\frac{\partial}{\partial t} + 1\right)^2 - l^2\nabla^2, \tag{4}$$

where $\gamma = v/l$ is the cortical damping rate in s^{-1}, v the axonal propagation velocity in m/s, and l the characteristic axonal length of cortical pyramidal neurons in m (Robinson et al., 1997). Thus, $\phi_e(x, t)$ denotes the incoming firing-rate to cortical neurons, at position x and time t, due to spreading of the activity of distant pyramidal neurons. It is this quantity that is approximately proportional to the EEG (Rennie et al., 2002). The strength of synaptic connections from neurons of type a to neurons of type b is denoted by ν_{ba} and is measured in mVs (Robinson et al., 1997). Fig. 2 provides an illustration of the anatomical connections incorporated into the model. The equations governing the models' dynamics are given in Appendix A. We use the nominal parameter values from (Robinson et al., 2002) displayed in Table 1 as the baseline condition, since they previously were identified with eyes-closed alert wakefulness which is dominated by spontaneous alpha oscillations.

Modeling the action of propofol

The most relevant targets of propofol are ligand-gated ion channels. Propofol is known to target γ-aminobutyric acid receptors of type A ($GABA_A$) as well as glutamergic (AMPA and NMDA) receptors. Its effect on $GABA_A$ receptors however, is much larger than its effect on both AMPA and NMDA receptors (Rudolph and Antkowiak, 2004) and we will therefore concentrate on these. The binding of propofol molecules to $GABA_A$ receptors leads to potentiation of GABA-gated chloride currents by decreasing the time constant of receptor deactivation (Rudolph and Antkowiak, 2004). Reports on the strength of potentiation highly differ between studies, most likely due to differences in receptor subtypes and experimental procedures. It is known for example, that the time-course of GABA perfusion determines the measured potentiation effects (Bai et al., 1999). While Adodra and Hales (1995) and Whittington and Jefferys (1996) report relative increases in potentiation of inhibitory postsynaptic currents and peak-amplitudes of up to 600%, Bai et al. (1999) and Kitamura et al. (2003) found that potentiation increased by at most 60% and peak-amplitudes remained unchanged (Kitamura et al., 2003) or increased only slightly (Bai et al., 1999) although the propofol concentrations in these studies are comparable (1–10 μM). Although propofol is known to target $GABA_A$ receptors, which can be found in both cortical and thalamic tissue (Kandel et al., 2000), there exist over a dozen receptor subtypes (McKernan, 1996) with largely unknown regional, cellular, and subcellular distributions (Sieghart and Sperk, 2002). Moreover, although propofol has been shown to possess a differential affinity for $GABA_A$ receptor subtypes, a complete characterization has not been realized (Jurd et al., 2003; Krasowski et al., 1998; Rudolph and Antkowiak, 2004).

To incorporate the above discussed physiology into the model, we note that since $GABA_A$ receptors mediate most of the inhibitory synaptic transmission within cortex as well as from reticular neurons to

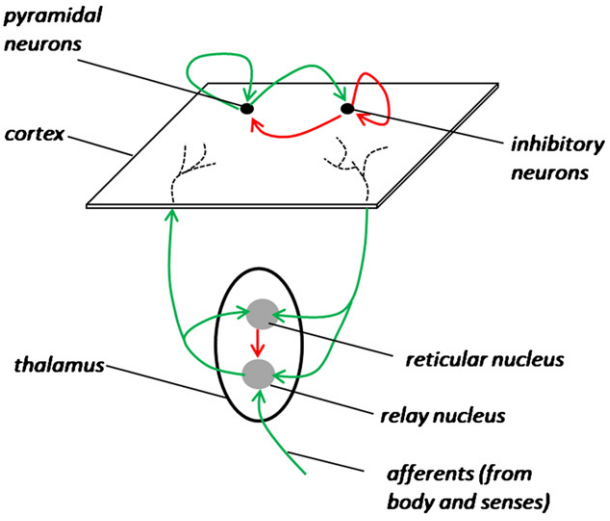

Fig. 2. Model connectivity. Shown are the four neuron types within the thalamo-cortical meanfield model (cortical pyramidal neurons, cortical inhibitory neurons, reticular nucleus, and thalamo-cortical relay neurons) together with their anatomical connections.

Table 1
Model parameters, their symbols, and nominal values (see Robinson et al., 2002).

Parameter	Symbol	Nominal value
Maximal firing-rate	Q_{max}	250 Hz
Average spike-threshold	θ	15 mV
Spike-threshold deviation	σ	3.3 mV
Synaptic decay rate	α	50 s^{-1}
Synaptic rise rate	β	200 s^{-1}
Synaptic strength from e to e neurons	ν_{ee}	1.2 mVs
Synaptic strength from i to e neurons	ν_{ei}	−1.8 mVs
Synaptic strength from s to e neurons	ν_{es}	1.2 mVs
Synaptic strength from i to i neurons	ν_{ii}	−1.8 mVs
Synaptic strength from e to i neurons	ν_{ie}	1.2 mVs
Synaptic strength from s to i neurons	ν_{is}	1.2 mVs
Synaptic strength from r to s neurons	ν_{sr}	−0.8 mVs
Synaptic strength from e to s neurons	ν_{se}	1.2 mVs
Synaptic strength from s to r neurons	ν_{rs}	0.2 mVs
Synaptic strength from e to r neurons	ν_{re}	0.4 mVs
Average noise level	$\nu_{sn}\langle\phi_n\rangle$	1 mV
Noise standard deviation	σ_n	0.1 mV
Cortico-thalamic delay	τ	80 ms
Cortical damping rate	γ	100 s^{-1}

neurons within thalamo-cortical relay nuclei, (Kandel et al., 2000) (apart from metabotropic $GABA_B$ receptors, which are not included into the model), all inhibitory synaptic contacts within the model are assumed to be mediated by $GABA_A$ receptors. To take into account the differential sensitivity of propofol to $GABA_A$ receptor subtypes, we distinguish between the inhibitory synaptic responses $\bar{h}$ of the different neuron types. Thus, we denote $\bar{h}_{ab}$ for the synaptic response of neurons of type a due to incoming firing rates of neurons of type b. In accordance with the above described experimental observations (Bai et al., 1999; Kitamura et al., 2003) and following Hutt and Longtin (2010), we model the action of propofol as a potentiation of the inhibitory synaptic responses $\bar{h}_{ii}$, $\bar{h}_{ei}$, and $\bar{h}_{sr}$. Formally, the administration of propofol leads to a percentile increase $p_k \geq 1$ in the decay time constant of $GABA_A$ receptors—or, equivalently, an equal decrease in the decay rate constant α_{ak}—located on neurons of type $k = i, e, s$:

$$\alpha_{ak} \to \alpha_{ak}/p_k. \tag{5}$$

While Hutt and Longtin (2010) chose $p_i = p_e$, reflecting equal affinity of propofol for $GABA_A$ receptors located on cortical inhibitory and pyramidal neurons, we relax this assumption, thereby accounting for the possibly differential affinity of propofol for different neuron types. Thus, taking p_i as reference, we parametrize p_e and p_s by

$$p_k = 1 + \epsilon_k(p_i - 1), \tag{6}$$

for $k = e, s$. The constants ϵ_e and ϵ_s are non-negative and dimensionless and serve to model the differential affinity of propofol for $GABA_A$ receptors located on the dendrites of neurons of type e and s, respectively, relative to its affinity for cortical inhibitory neurons. For example, $\epsilon_s = 0$ reflects a complete insensitivity of propofol for $GABA_A$ receptors on thalamo-cortical relay neurons, and $\epsilon_e = 1$ reflects an equal affinity of propofol for $GABA_A$ receptors on cortical pyramidal and inhibitory neurons.

The action of propofol is modeled as a decrease in the decay rate of the $GABA_A$ receptors and does not influence their *efficacy*, that is, the maximum chloride current upon receptor activation, in agreement with experimental observations (Kitamura et al., 2003). Since in the model, synaptic efficacy is proportional to the maximum value η of $\bar{h}$, which is given by

$$\eta(\alpha,\beta) = \frac{\alpha\beta}{\beta-\alpha}\left[exp\left(-\alpha\frac{ln(\beta/\alpha)}{\beta-\alpha}\right) - exp\left(-\beta\frac{ln(\beta/\alpha)}{\beta-\alpha}\right)\right], \tag{7}$$

the maximum height of $\bar{h}$ depends on the rate constants α and β. In particular, by parametrizing synaptic responses by $\bar{h}$, propofol-induced changes in the decay rate α indirectly change the efficacy of the synapse, which needs to be compensated for. This is not a fundamental issue but a technical one and can be accounted for by re-parametrizing synaptic responses in such a way that changes in α (and/or β) do not influence their maximal heights (Hutt and Longtin, 2010). See (Bojak and Liley, 2005) for a similar re-parametrization in the context of modeling the synaptic action of the anesthetic agent isoflurane. Thus, we replace the synaptic response $\bar{h}$ by h, which is defined as

$$h(t) = \frac{H}{\eta(\alpha,\beta)}\bar{h}(t), \tag{8}$$

where we introduce H as the synaptic efficacy. Note that the maximum height of h indeed equals H and hence is independent of the rate constants α and β. Since the chosen baseline values for α and β (see Table 1) give a value of $\eta(\alpha, \beta) \approx 31.5\ s^{-1}$ we set $H = 31.5\ s^{-1}$. Fig. 3(a) shows how h varies with the factor p. Thus, while the rise-rate and efficacy of h remain unaltered, its response is prolonged, reflecting a decrease in α. Fig. 3(b) shows how the spectral power of h varies with the factor p. It illustrates that the administration of propofol leads to enhanced synaptic selectivity for low-frequency pre-synaptic input.

Theoretical EEG power spectrum

In this section we derive a formula for the transfer function from ϕ_n to ϕ_e. Since ϕ_e is approximately proportional to the EEG (Rennie et al., 2002) we take the derived power spectrum as a model for the experimentally observed EEG power spectrum. We point out that in other meanfield studies, not ϕ_e, but instead the mean soma voltage V_e is taken to be proportional to the EEG (Liley and Cadusch, 2002; Nunez and Srinivasan, 2006). In the linear regime however, and for spatially-homogeneous dynamics, ϕ_e and V_e are approximately proportional for frequencies that are small as compared to the cortical damping rate γ (as in the present study). Thus, the results will not crucially depend on this choice. The transfer function contains all information on the linearized dynamics of ϕ_e. Since spontaneous EEG activity under physiological conditions is dominated by linear fixed-point dynamics (Hindriks et al., 2011; Stam et al., 1999), the transfer function should be adequate in the present context.

The transfer function from ϕ_n to ϕ_e can be expressed in terms of the frequency responses between the different neuron types. For pairs of neuron types (a,b) that are located either within cortex or within thalamus, that is, for $(a, b) \in \{(e, e), (e, i), (i, e), (i, i), (r, s), (s, r)\}$, the frequency response from neurons of type b to neurons of type a is given by

$$\zeta_{ab}(\omega) = \frac{H}{\eta}\nu_{ab}S'(V_a^*)\left(1+\frac{i\omega}{\alpha_{ab}}\right)^{-1}\left(1+\frac{i\omega}{\beta_{ab}}\right)^{-1}, \tag{9}$$

where ω denotes complex angular frequency, S' denotes the derivative of the activation function S with respect to the voltage V_a, and V_a^* denotes the steady-state value of V_a. For pairs of neuron types (a, b) for which one type is located in cortex and the other in thalamus, that is, for $(a, b) \in \{(e, s), (i, s), (r, e), (s, e)\}$, the frequency response from neurons of type b to neurons of type a contains a phase shift that is due to the propagation delay $\tau/2$ between cortex and thalamus and is given by

$$\zeta_{ab}(\omega) = \frac{H}{\eta}\nu_{ab}S'(V_a^*)\left(1+\frac{i\omega}{\alpha_{ab}}\right)^{-1}\left(1+\frac{i\omega}{\beta_{ab}}\right)^{-1}e^{-i\omega\tau/2}. \tag{10}$$

The above frequency responses can be combined into frequency responses of the different anatomical loops making up the thalamo-cortical system. We write $\zeta_{abc}(\omega)$ for the combined frequency response $\zeta_{ab}(\omega)\zeta_{bc}(\omega)$ for $a, b, c \in \{e, i, r, s\}$. Thus, for example, $\zeta_{ese}(\omega) =$

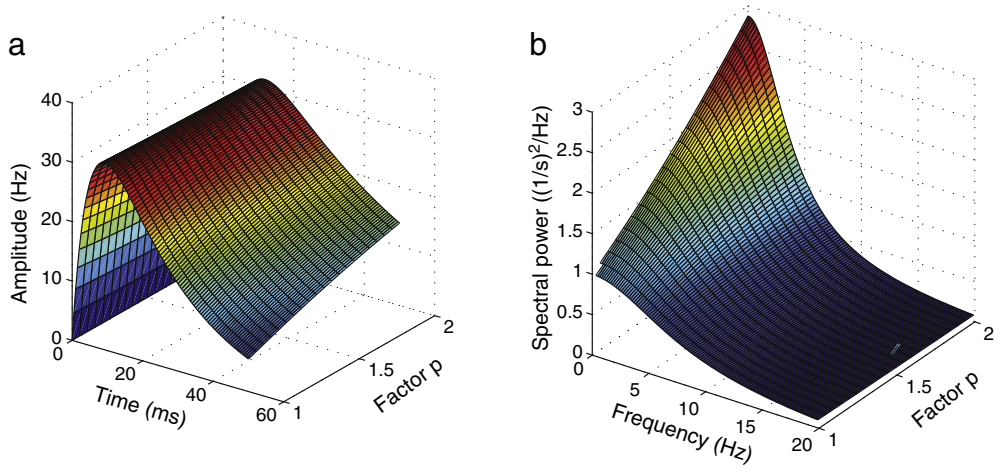

Fig. 3. Effect of propofol on the dynamics of GABA-ergic synapses. The figures illustrate the effect of increasing the factor p on the response of GABA-ergic synapses. In (a) the synaptic response function h is plotted as a function of time and p and in (b) the Fourier transform of h is plotted as a function of frequency and p.

$\zeta_{es}(\omega)\zeta_{se}(\omega)$ denotes the frequency response of the excitatory thalamic-cortico-thalamic loop. When individual frequency responses are combined into a loop, we refer to the combined frequency response as *feedback* within this loop.

In Appendix B we derive that the transfer function from ϕ_n to ϕ_e is given by

$$\frac{\phi_e}{\phi_n} = \frac{\zeta_{eisn} + (1-\zeta_{ii})\zeta_{esn}}{[(D-\zeta_{ee})(1-\zeta_{srs})-\zeta_{ese}-\zeta_{esre}](1-\zeta_{ii})-\zeta_{eie}(1-\zeta_{srs})-\zeta_{eise}-\zeta_{eisre}}, \tag{11}$$

where $D=(1+i\omega/\gamma)^2+r^2\|\mathbf{k}\|^2$ denotes the wave operator in $(\mathbf{k}, \omega)$-space where $\mathbf{k}=(k_1, k_2)$ denotes a pair of wavenumbers. Fig. 4 provides an illustration of the anatomical loops whose feedbacks determine the transfer function. If we assume random connectivity ($v_{ik}=v_{ek}$ for $k\in\{e, i, s\}$) and all synaptic responses to be equal, (11) reduces to the formula derived in Rennie et al. (2002). The dispersion relation corresponding to (11) is obtained by setting its denominator to zero, hence is given by

$$[(D-\zeta_{ee})(1-\zeta_{srs})-\zeta_{ese}-\zeta_{esre}](1-\zeta_{ii})-\zeta_{eie}(1-\zeta_{srs}) = \zeta_{eise}+\zeta_{eisre}. \tag{12}$$

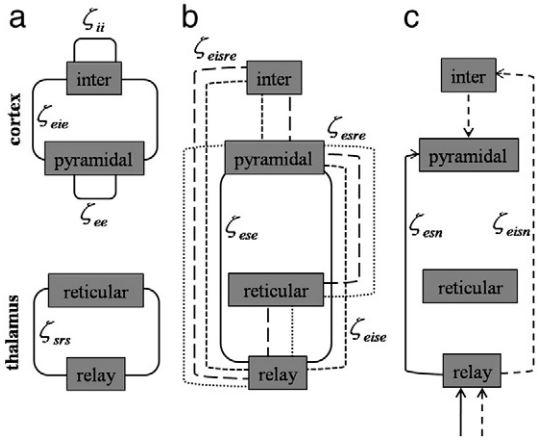

Fig. 4. Feedbacks within the thalamo-cortical system. The figure shows the different feedback loops within the thalamo-cortical meanfield model. (a) Intra-cortical and intra-thalamic loops, (b) thalamo-cortico-thalamic loops, and (c) feedforward pathways. The frequency responses of these feedback loops and feedforward pathways determine the transfer function from ϕ_n to ϕ_e and hence the theoretical EEG power spectrum.

A solution $(\mathbf{k}, \omega)$ of (12) corresponds to a thalamo-cortical resonance with wavenumbers $\mathbf{k}$, damping rate $\mathrm{Im}(\omega)$, and angular frequency $\mathrm{Re}(\omega)$. Thus, stable resonances are characterized by $\mathrm{Im}(\omega)<0$ while unstable resonances have $\mathrm{Im}(\omega)>0$ and correspond to limit-cycle dynamics.

Following Robinson et al. (2002) we restrict attention to spatially-homogenous dynamics ($\mathbf{k}=(0, 0)$) since it simplifies the analysis of the dispersion relation. The exact shape of the theoretical power spectrum matters when parameters are derived directly from EEG data as in Rowe et al. (2004), but the overall spectrum changes induced by parameter variations are dominated by the spatially-homogenous solutions (Robinson et al., 2001). Under the assumption of spatial-homogeneity, the theoretical EEG power spectrum is given by

$$P(\omega) = \sigma_n^2|\phi_e(\omega)|^2, \tag{13}$$

where the vertical bars mean absolute value and σ_n^2 denotes the variance of the noise term ϕ_n (see Table 1). Although propofol-induced alpha oscillations are not equally strong over the entire cortex, they can be recorded from every electrode and have a high degree of spatial coherence (Cimenser et al., 2011). This makes the restriction to spatially-homogeneous dynamics at least partially justified. In any case, successful reproduction of the discussed EEG phenomenology does not depend on the exact formula for the theoretical EEG power spectrum.

Results

Reproduction of experimental observations

In this section we show that the model is able to reproduce the EEG phenomenology described in Section 2.1. namely, increases in delta and theta power and more pronounced alpha oscillations with increased peak-frequency. We first evaluated whether the observed increases in delta and theta power and in alpha peak-frequency are statistically significant on the group-level. For every subject and in both the baseline and anesthesia condition, we computed the power spectra using Welch's averaging method with two-second windows with 50% overlap. From these spectra we compute delta (0.5–3 Hz) and theta power (3–6 Hz) and alpha peak-frequencies. To assess statistical significance we used a permutation test. Thus, we randomly partitioned all selected subjects into two classes and for each class computed the above statistics (delta power, theta power, and alpha peak-frequency). By repeating this procedure 1000 times, a surrogate distribution is created under the null hypothesis of no differences

between baseline and anesthesia conditons. p-Values are defined through the ranking of the experimentally observed statistics-values within the surrogate distribution. Power within the delta and theta bands increased under anesthesia as compared to baseline ($p<0.05$). Moreover, alpha peak-frequency shifted from 8.5 Hz (std 0.9 Hz) in baseline to 9.9 Hz (std 1.2 Hz) under anesthesia ($p<0.05$). Fig. 5(a) shows the group-averaged EEG power spectra in both conditions and Fig. 5(b) shows the EEG power spectra of a single subject.

By lack of physiological data we initially set $\epsilon_e = {}_s$, reflecting equal affinity of propofol for $GABA_A$ receptors located on excitatory neurons (cortical pyramidal neurons and thalamo-cortical relay neurons). As we will see in Section 3.3 this choice is not essential for reproducing the EEG phenomenology. Moreover we choose ϵ_e, ${}_s<1$, reflecting a greater affinity of propofol for $GABA_A$ receptors located on cortical inhibitory neurons than for $GABA_A$ receptors located on excitatory neurons. This assumption is essential for reproducing the EEG phenomenology and we will discuss it further in Section 3.3. We set $\epsilon_e = \epsilon_s = 0.5$. Fig. 5(c) shows the theoretical EEG power spectra in the baseline condition ($p_i = 1$) and after the administration of propofol ($p_i = 1.15$). The figure shows that the model responds similarly as the human frontal cortex. Specifically, it displays increases in delta and theta power as well as more pronounced alpha oscillations with increased peak-frequency. Although the increase in alpha peak-frequency (0.38 Hz) is less than the average increase observed in the data, it falls within the experimentally observed range. Figs. 5(d) and (f) show EEG time-series recorded from electrode Fz of a single subject in baseline and under anesthesia, respectively, while Figs. 5(e) and (g) show corresponding simulated EEG time-series. The experimentally observed increases in low-frequency power and more pronounced alpha oscillations are visible in the simulated time-series as well.

Amplification of thalamo-cortical resonances

We now analyze how the dynamics within the thalamo-cortical system is altered by the action of propofol. To this end we employ the dispersion relation (12). Numerically solving (12) shows that in baseline, there exist three thalamo-cortical resonances within the relevant frequency band (that is, up to and including the alpha band). First, we observe an oscillatory resonance with a frequency of about ~8 Hz. This resonance is identified with spontaneous alpha oscillations observable during relaxed wakefulness (Robinson et al., 2001, 2002; Rowe et al., 2004). We will refer to this resonance as the *alpha resonance*. The alpha resonance is reflected in the EEG power spectrum as a peak near 8 Hz as Fig. 6(a) illustrates. Second, a pair of zero-frequency resonances (that is, with $\omega = 0$) is present. These resonances underlie the EEG background spectrum from which oscillatory resonances emerge (Robinson et al., 2001). Figs. 6(b) and (c) show how the damping-rate and frequency of these resonances are modulated by the administration of propofol. With increasing propofol concentration, the damping of the alpha resonance weakens (Fig. 4(b)) while its frequency increases (Fig. 6(c)). These modulations

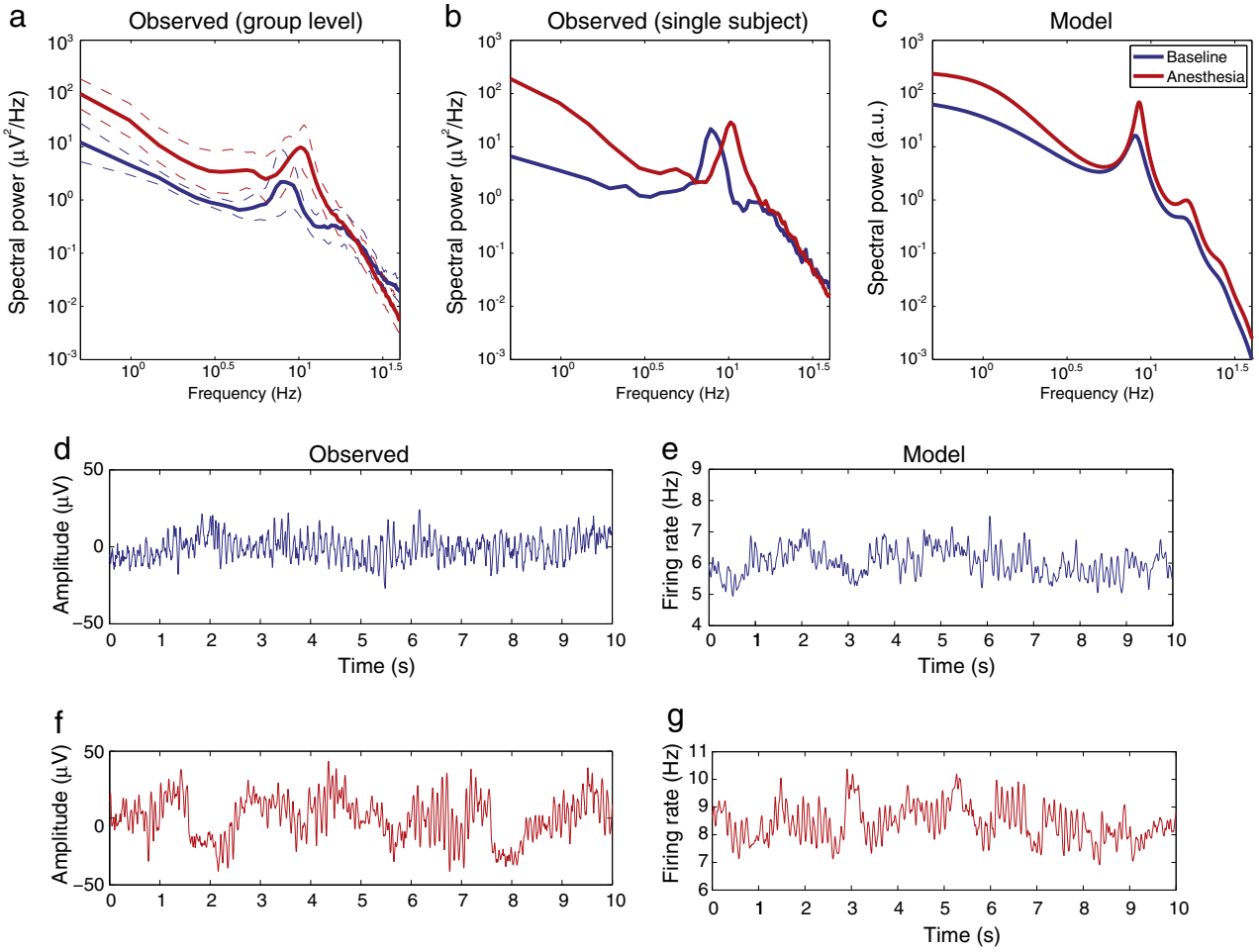

Fig. 5. Observed and modeled EEG. (a) Group-averaged EEG power spectra in the baseline condition (solid blue line) and in the anesthesia condition (solid red line). The dashed lines denote the respective standard deviations. (b) EEG power spectra of a single subject. (c) Theoretical EEG power spectrum in the baseline condition (blue) and in the anesthesia condition (red) ($p_i = 1.15$, $\epsilon_e = \epsilon_s = 0.5$). (d) and (f) show 10-second time series of EEG recorded from a single subject in the baseline and anesthesia condition, respectively. (e) and (g) show ten-second time series of simulated EEG in the baseline and anesthesia condition, respectively ($p_i = 1.15$, $\epsilon_e = \epsilon_s = 0.5$).

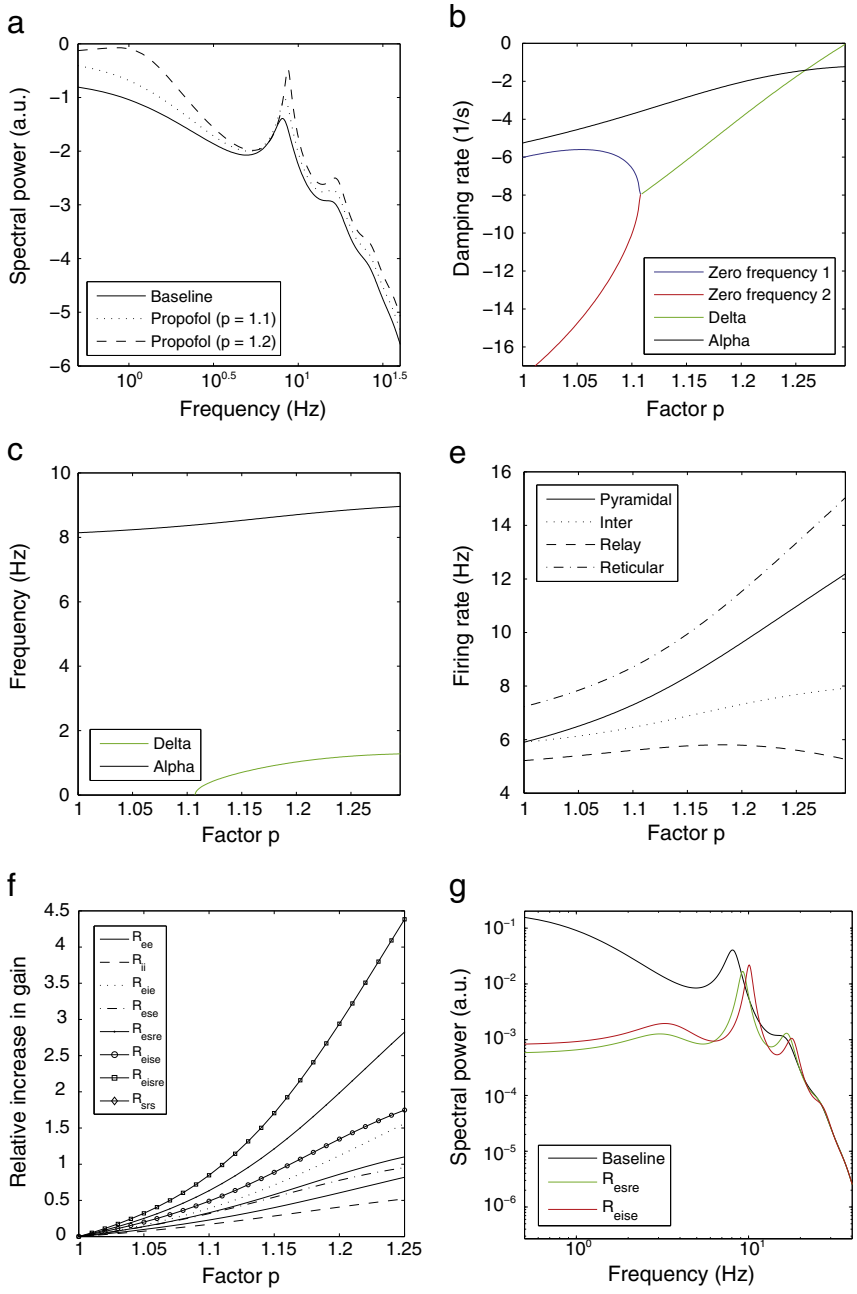

Fig. 6. Modulation of resonances and firing-rates. Shown are the damping rates (b) and frequencies (c) of the thalamo-cortical resonances as a function of the percentile increase in the time constant of GABA-ergic receptors on cortical inhibitory neurons (p_i). The differential affinities $_e$ and $_s$ were both set to 0.5. (a) shows theoretical EEG power spectra in the baseline condition ($p_i = 1$) and for $p_i = 1.1$ and $p_i = 1.2$. (d) Steady-state firing rates of the different neuron types as functions of propofol concentration.

in damping and frequency of the alpha resonance underlie the increase in alpha power and peak-frequency respectively (Fig. 6(a)). Furthermore, the pair of zero-frequency resonances collides and gives way to a *delta resonance* that gradually increases in frequency but saturates at about 1 Hz. This is reflected in the EEG power spectrum by increases in delta and theta power and finally the appearance of a spectral peak in the delta band (Fig. 6(a)). The delta resonance might by related to slow-frequency oscillations that can be observed during deeper levels of anesthesia (San-juan et al., 2010). In this study however, we will not consider it further.

Fig. 6(d) shows the steady-state firing rates of the different neuron types as functions of the factor p, which were computed by numerically solving the steady-state equations derived in Appendix C. While the administration of propofol has relatively little effect on the firing rates of cortical inhibitory neurons and thalamo-cortical relay neurons, cortical pyramidal neurons as well as thalamic reticular neurons exhibit increased firing rates. Since the steady-state voltages $V_a^* = S^{-1}(Q_a^*)$ are typically smaller than the average activation threshold θ, increased steady-state firing rates Q_a^* lead to increased excitabilities $S'(V_a^*)$, and hence to increased frequency responses (9). The increased frequency responses on their part, lead to enhanced feedback within all loops making up the thalamo-cortical system, thereby amplifying the thalamo-cortical resonances according to the dispersion relation (12). Fig. 6(e) shows the relative increases $R_l(p)$ in the feedbacks within the different anatomical loops l of the thalamo-cortical system, as a function of the factor p. Thus, $R_l(p)$ is defined by

$$R_l(p) = \frac{|\xi_l^p(0)| - |\xi_l^0(0)|}{|\xi_l^0(0)|}, \tag{14}$$

where $l \in \{ee, ii, eie, ese, esre, eise, eisre, srs\}$ denotes the anatomical loop and $\xi_l^0(0)$ and $\xi_l^p(0)$ denote the frequency-independent (that is, computed in $\omega = 0$) feedbacks in l in the baseline condition ($p = 0$) and during anesthesia (corresponding to the factor p), respectively. Selectively increasing the feedbacks in the dispersion relation (12) uncovers that only increases in *negative thalamo-cortico-thalamic feedback* ($l = esre$ or $l = eise$) lead to increased alpha peak-frequencies. This is illustrated in Fig. 6(f) which shows theoretical EEG power spectra in baseline condition and for increased R_{esre} and R_{eisre} (corresponding to $p = 1.25$). Notice the increase in alpha peak-frequency.

Essential role of local cortical inhibitory networks

What are the differential roles of potentiation of $GABA_A$ receptors located on the dendrites of different neuronal types? If we specifically target $GABA_A$ receptors located on cortical pyramidal neurons (by decreasing α_{ei} while keeping α_{ii} and α_{sr} unaffected) the simulated EEG shows an overal decrease in power and attenuation of alpha oscillations. The same can be observed when we specifically target receptors on thalamo-cortical relay neurons. In contrast, if we specifically target $GABA_A$ receptors located on cortical inhibitory neurons, increases in delta and theta power as well as pronounced alpha oscillations are observed. Thus, $GABA_A$-ergic potentiation within local cortical interneuron networks suffices to invoke the experimentally observed EEG phenomenology. Moreover, when propofol is unselectively administered to cortical and thalamic tissue—as is likely to be the case in clinical practice—the experimentally observed EEG phenomenology is reproduced only if the affinity of propofol for $GABA_A$ receptors on cortical inhibitory neurons is sufficiently higher than its affinity for cortical pyramidal neurons. Formally, this means that γ_e has to be sufficiently smaller than 1. Fig. 7(a) shows theoretical EEG power spectra for $\epsilon_e = 0.3$ and for $\epsilon_e = 0.7$ (we now have relaxed the assumption $\epsilon_e = \gamma_s$ and chosen $\epsilon_s = 1$). For each of these values, three spectra are plotted, corresponding to different levels of the factor p_i. As the figure shows, the EEG phenomenology is reproduced for $\epsilon_e = 0.3$ but not for $\epsilon_e = 0.7$. As Fig. 7(b) shows, variations in ϵ_s linearly modulate the threshold of ϵ_e for the emergence of the experimentally observed EEG phenomenology. These observations show that the pronounced alpha oscillations, together with increased delta and theta power can be robustly generated by the model and are caused by increased inhibition within local inhibitory interneuron networks. We note that, for given ϵ_s, there exists a small range of values of ϵ_e for which increases in delta and theta power are observed while alpha oscillations are not enhanced and can even be attenuated. Thus, using different parameter settings, the model reproduces the EEG phenomenology that is typically observed over occipital and parietal regions, namely, increased delta and theta power and simultaneous attenuation of alpha oscillations.

Discussion

Main findings

In this study we employed a meanfield model of the thalamo-cortical system (Rennie et al., 2002; Robinson et al., 2001) to elucidate the mechanisms underlying the EEG changes observed during the maintenance period of propofol-induced general anesthesia. We have shown how the action of propofol can be incorporated into the model, taking into account the possible differential affinity of propofol for different neuron types, and derived a general formula for the theoretical EEG power spectrum. We compared the model predictions with EEG data obtained from subjects scheduled for surgery for which propofol was used as the general anesthetic. The model reproduced the experimentally observed EEG changes within different frequency bands, namely, increases in delta and theta power, and pronounced alpha oscillations with increased peak-frequency. Moreover, we elucidated the suggested physiological mechanisms underlying these changes. The modeling carried out in this study demonstrates that propofol-induced EEG changes can be understood in terms of the macroscopic properties of the thalamo-cortical system.

The modeling carried out in this study suggests the following mechanisms to underlie the observed EEG changes. Potentiation of $GABA_A$ receptors located on the dendrites of cortical interneurons increases inhibition within these networks, thereby dis-inhibiting cortical pyramidal neurons. Increased activity of cortical pyramidal neurons spreads throughout the thalamo-cortical system via intracortical, cortico-thalamic, and intra-thalamic projections. This results in increased firing rates of cortical pyramidal neurons and thalamic reticular, thereby enhancing feedback within all anatomical loops making up the thalamo-cortical system. The enhanced feedbacks lead to amplification of the thalamo-cortical resonances which are reflected in the EEG. Specifically, increased delta power is a reflection of the amplification of a non-oscillatory resonance (actually a pair of resonances). Likewise, the pronounced alpha oscillations reflect the amplification of the underlying oscillatory resonance within the alpha band (the alpha resonance), which was previously identified with

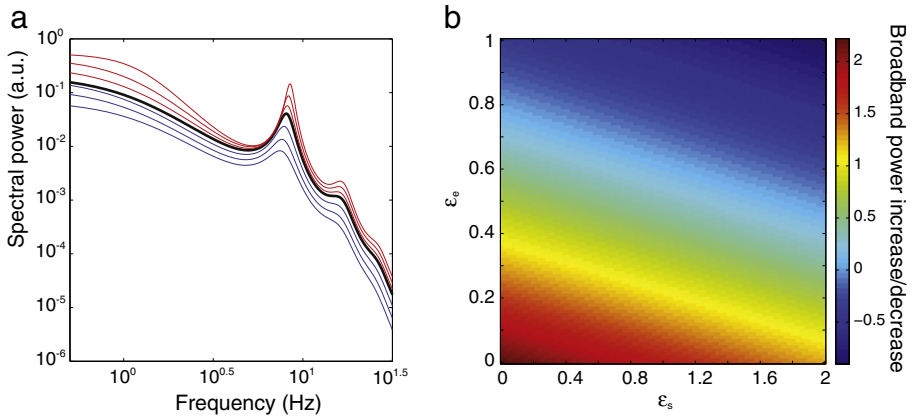

Fig. 7. Parameter-dependence of propofol-induced EEG rhythms. (a) Theoretical EEG power spectra in baseline (black line) and for three increasing values of p_i for $\gamma_e = 0.3$ (red solid lines) and $\gamma_e = 0.7$ (blue solid lines). In both cases $\gamma_s = 1$. (b) Color-coded increases/decreases in broadband EEG power due to a small increase in p_i ($p_i = 1.02$), compared to baseline ($p_i = 1$) as a function of the differential affinities γ_e and γ_i. Values > 0 correspond to pairs (γ_e, γ_i) for which the model reproduces the experimentally observed EEG phenomenology, while values < 0 correspond to pairs (γ_e, γ_i) for which the model shows an overall decrease in broadband EEG power.

spontaneous alpha oscillations during relaxed wakefulness (Robinson et al., 2001, 2002; Rowe et al., 2004). In contrast to the delta and alpha bands, the modeling carried out in this study suggests that increased theta power might not be due to the modulation of an underlying thalamo-cortical resonance within the theta band. Instead, it is understood as a side-effect of the amplification of the zero-frequency and alpha resonances, which leak spectral energy into the theta band. Some indirect support for this interpretation is given by the fact that in the data relative increases in delta power are higher than the relative increases in theta power. Concerning the increase in alpha peak-frequency, we found that it is caused by enhanced negative feedback between cortex and thalamus.

Scope and extensions

Besides propofol, there exist several other anesthetic agents such as the ethers isoflurane and sevoflurane that cause potentiation of $GABA_A$ receptors (Rudolph and Antkowiak, 2004). The EEG phenomenology focused on in this study, namely, strong frontal alpha oscillations, together with increased delta and theta power, is also observed during general anesthesia induced by sevoflurane (Gugino et al., 2001). This provides indirect evidence that the observed EEG phenomenology is indeed caused by the potentiation of $GABA_A$ receptors, and not by modifications in other receptor types that are targeted by these anesthetic agents. We note though, that there also exist differences in spontaneous EEG activity induced by propofol, sevoflurane, and isoflurane (Schwender et al., 1996). Presumably, the precise character of the induced EEG activity depends on the interplay between the different receptors that are targeted, in combination with the distinct affinity of these substances for different receptor subtypes (Rudolph and Antkowiak, 2004).

Existing applications of neural meanfield models to anesthesia-induced changes in spontaneous EEG rhythms mostly focused on understanding the dynamical mechanisms underlying bi-phasic responses (Bojak and Liley, 2005; Hutt and Longtin, 2010; Steyn-Ross et al., 1999). In Steyn-Ross et al. (1999) a reduced version of the cortical meanfield model (Liley and Cadusch, 2002) is used to show that the bi-phasic response can be understood as a thermodynamic phase transition in which the cortex abruptly jumps from a highly-activated equilibrium state to a state in which cortical activity is suppressed. Alternatively, in Bojak and Liley (2005) the general model equations (Liley and Cadusch, 2002) are used to argue that bi-phasic responses can be understood without bistability. The authors show that bi-phasic responses can be generated about a single stable equilibrium state. In Hutt and Longtin (2010) a simplified cortical meanfield model is used to demonstrate analytically that bi-phasic responses are a general property of neural meanfields comprising excitatory and inhibitory neurons types, linear synaptic dynamics, and non-linear activation functions. Moreover, in the simplified model, bi-phasic responses could be observed on different stable branches of cortical equilibrium points, as well as during jumps between different stable branches, thereby linking previous approaches.

In contrast to the above mentioned studies, which concentrated on the mechanisms underlying bi-phasic responses, in the current study we concentrated on reproducing the detailed spectral EEG changes observed during the first phase of the bi-phasic response induced by propofol, which is characterized by an increase in power, including the alpha rhythm, with increased peak-frequency. Thus, while the current study reproduces the spectral EEG changes induced by propofol in more detail than (Hutt and Longtin, 2010) which did not focus on reproducing spectral EEG peaks themselves, but instead on bi-phasic power changes, it is limited to the first phase of the bi-phasic response. This relatively good agreement with the exact shape of the EEG power spectra during the first phase of the bi-phasic response suggests that thalamic feedback could be essential for generating the complete bi-phasic response. To study this issue further however, requires examination of the model's dynamics for higher propofol concentrations. Preliminary simulations already showed that—depending on the exact parameter settings—different instabilities can occur including Hopf instabilities of the delta and alpha resonances, as well as jumps to a different stable branch of thalamo-cortical equilibria. Pursuing this direction will be the topic of future research.

Model predictions

The increased mean firing rates of cortical pyramidal neurons observed in our model in response to the administration of propofol (see Fig. 6(d)) may seem to contrast the decreased firing rates reported in previous modeling studies (Bojak and Liley, 2005; Hutt and Longtin, 2010; Steyn-Ross et al., 1999) and observed in experiments (Antkowiak, 1999). The increased firing rates in our model most likely directly relate to the increased frequencies of the thalamo-cortical resonances. This also makes sense from an electrophysiological point of view; an increased frequency of macroscopic neuronal oscillations reflects reduced interburst intervals of the periodically bursting neurons in the underlying population, which also increases their mean firing rate. However, in contrast to our study Steyn-Ross et al. (1999), Bojak and Liley (2005) and Hutt and Longtin (2010) did not observe increased EEG frequencies. Specifically, the reduced model studied in Steyn-Ross et al. (1999) does not display oscillations and in Bojak and Liley (2005) a *decrease* in alpha peak-frequency was found, rather than an *increase*, consistent with the reduced firing rates observed in their study. The same holds for the reduced firing rates observed experimentally in rat neocortical slice preparations; these are due to increased interburst intervals of periodically bursting pyramidal neurons (Antkowiak, 1999) hence are associated with *slowing* of neuronal oscillations. These considerations resolve the apparent discrepancy between our findings and earlier studies. Presumably, experimental backup for the increased firing rates observed in our model must come from thalamo-cortical preparations in which increased alpha peak-frequencies can be observed for relatively low propofol concentrations, corresponding to the first phase of the bi-phasic response.

The modeling carried out in this study leads to several predictions that can in principle be experimentally verified. First, an essential role for local cortical inhibitory networks is suggested. Specifically, the modeling predicts that propofol has a higher affinity for $GABA_A$ receptor subtypes located on cortical interneurons than for $GABA_A$ receptor subtypes located on cortical pyramidal neurons. This implies a differential cellular distribution of $GABA_A$ receptor subtypes, for which there is experimental evidence (Xiang et al., 1998). However, since the mammalian cortex contains several types of inhibitory interneurons (Kandel et al., 2000) which are lumped together in the model (Robinson et al., 1997), no predictions can be made on the differential sensitivity of propofol for the different types of interneurons. Interestingly, Liley et al. (2003) employed a different neural meanfield model (Liley and Cadusch, 2002) which led to the same prediction for the differential action of benzodiazepines, for which direct experimental support was available. Second, and in connection with this, the modeling suggests that the observed EEG changes crucially depend on the binding of propofol to $GABA_A$ receptors located on cortical interneurons. The modeling therefore predicts that selective administration of propofol to cortical interneuron networks will lead to the discussed EEG phenomenology. Third, since the modeling interprets the EEG changes as reflections of amplified thalamo-cortical resonances, it predicts increased coherences between the relevant parts of the frontal cortex and thalamic nuclei, especially within the alpha frequency band. This increased coherence through alpha resonance might relate to unconsciousness by prohibiting localized processing in frontal cortex as well as blocking integration of information between different parts of the cortex (Alkire et al., 2008).

Limitations

Although the model used in this study qualitatively reproduces the discussed EEG phenomenology, there are some quantitative differences. First, the model is relatively sensitive to propofol; while several studies point towards GABA-ergic potentiation of at least 60% at clinically relevant concentrations (Bai et al., 1999; Kitamura et al., 2003), our modeling suggests potentiation of about 10%. This discrepancy most likely is caused by our choice of baseline, for which we used the nominal parameter values (see Table 1) that were previously identified with eyes-closed resting-state (Robinson et al., 2001, 2002; Rowe et al., 2004). However, since frontal alpha oscillations during wakefulness have relatively lower power and are less pronounced than parietal and occipital alpha oscillations, the baseline should be adjusted accordingly. Some preliminary simulations showed that the 10% increase in GABA-ergic potentiation can be changed by adjusting the baseline. A systematic investigation of this issue however, requires a global parameter search in the style of (Bojak and Liley, 2005) which is outside the scope of this study. We take it as an encouraging fact that, while using a baseline that is independently determined in previous investigations (Robinson et al., 2002; Rowe et al., 2004), the model's response is qualitatively similar to the response of the human frontal cortex.

Second, the model's increase in alpha peak-frequency is relatively modest as compared to the mean increase observed experimentally (although still within the experimentally observed range). Although the natural frequency of the alpha resonance keeps increasing at higher concentrations of propofol (see Fig. 6(c)), a better match with the data would be desirable. Again, this discrepancy might be resolved through a global parameter search for different baselines. Alternatively, since the alpha peak-frequency is partially determined by the delay-time between cortex and thalamus, another cause for the observed increase could be a propofol-induced acceleration of axonal propagation delays. However, there does not seem to be any experimental indication for such an effect. Besides these quantitative differences, the model does not display a transient increase in EEG beta power—so-called *paradoxical excitation*—which precedes the increase in alpha power discussed in this study (Gugino et al., 2001). Since spike-frequency adaptation is implicated to play a key role in the generation of this particular phenomenon (McCarthy et al., 2008), the inclusion of adaptation dynamics into the current meanfield model (Loxley and Robinson, 2007) might lead to an integrated understanding of a more broad spectrum of propofol-induced EEG phenomena. Despite this issues, the results reported in this study are encouraging and demonstrate that the discussed EEG phenomenology can be qualitatively reproduced by the used thalamo-cortical meanfield model, suggesting that it contains the essential physiological underlying mechanisms.

Appendix A. System equations

The average membrane potentials V_e, V_i, V_r, and V_s obey the following set of coupled equations:

$$V_e(x,t) = \bar{h}\otimes\nu_{ee}\phi_e(x,t) + \bar{h}\otimes\nu_{es}S(V_s(x,t-\tau/2)) + \bar{h}\otimes\nu_{ei}S(V_i(x,t)), \tag{15}$$

$$V_i(x,t) = \bar{h}\otimes\nu_{ie}\phi_e(x,t) + \bar{h}\otimes\nu_{is}S(V_s(x,t-\tau/2)) + \bar{h}\otimes\nu_{ii}S(V_i(x,t)), \tag{16}$$

$$V_s(x,t) = \bar{h}\otimes\nu_{sn}\phi_n(x,t) + \bar{h}\otimes\nu_{se}\phi_e(x,t-\tau/2) + \bar{h}\otimes\nu_{sr}S(V_r(x,t)), \tag{17}$$

$$V_r(x,t) = \bar{h}\otimes\nu_{rs}S(V_s(x,t)) + \bar{h}\otimes\nu_{re}\phi_e(x,t-\tau/2), \tag{18}$$

$$D(x,t)\phi_e = S(V_e(x,t)), \tag{19}$$

where t denotes time in sec, x denotes position on the cortical sheet, $\otimes$ denotes the convolution operator, and ϕ_n is non-specific input to thalamo-cortical relay neurons, which has the form $\phi_n = \langle\phi_n\rangle + \sigma_n\xi(t)$, where $\langle\phi_n\rangle$ denotes its mean value, $\xi(t)$ a unit-variance Gaussian white-noise process, and σ_n its standard deviation. The above system of equations can be rewritten as a set of ten coupled partial differential equations by rewriting the impulse response $\bar{h}$ as a second-order linear differential operator. In modeling the action of propofol, the impulse response $\bar{h}$ is replaced by its reparametrization h.

Appendix B. Derivation of the transfer function

In this Appendix we derive the transfer function from ϕ_n to ϕ_e of the dynamical system described by Eqs. (15)–(19) were we use the reparametrization h of the synaptic impulse responses. We denote the synaptic frequency response function from neurons of type b to neurons of type a by $L_{ab}(\omega)$, where ω denotes complex frequency and is given by the Fourier transform of h:

$$L_{ab}(\omega) = \frac{H}{\eta}\left(1+\frac{i\omega}{\alpha_{ab}}\right)^{-1}\left(1+\frac{i\omega}{\beta_{ab}}\right)^{-1}. \tag{20}$$

Rewriting Eqs. (15)–(19) in the $(\mathbf{k}, \omega)$-domain gives

$$V_e = L_{ee}\nu_{ee}\phi_e + L_{es}\nu_{es}Q_s e^{-i\omega\tau/2} + L_{ei}\nu_{ei}Q_i, \tag{21}$$

$$V_i = L_{ie}\nu_{ie}\phi_e + L_{is}\nu_{is}Q_s e^{-i\omega\tau/2} + L_{ii}\nu_{ii}Q_i, \tag{22}$$

$$V_s = L_{sn}\nu_{sn}\phi_n + L_{se}\nu_{se}\phi_e e^{-i\omega\tau/2} + L_{sr}\nu_{sr}Q_r, \tag{23}$$

$$V_r = L_{rs}\nu_{rs}Q_s + L_{re}\nu_{re}\phi_e e^{-i\omega\tau/2}, \tag{24}$$

$$D\phi_e = Q_e, \tag{25}$$

where $D = (1+i\omega/\gamma)^2 + r^2\|\mathbf{k}\|^2$ is the wave operator in the $(\mathbf{k}, \omega)$-domain. By linearizing S about a spatially-homogeneous steady-state $(V_e^*, V_i^*, V_r^*, V_s^*)$ of (V_e, V_i, V_r, V_s);

$$S(V_a) \approx S(V_a^*) + S'(V_a^*)V_a, \tag{26}$$

for $a \in \{e, i, r, s\}$ and by discarding constants, we can rewrite Eqs. (21)–(25) as

$$D\phi_e = \zeta_{ee}\phi_e + \zeta_{es}Q_s + \zeta_{ei}Q_i, \tag{27}$$

$$Q_i = \zeta_{ie}\phi_e + \zeta_{is}Q_s + \zeta_{ii}Q_i, \tag{28}$$

$$Q_s = \zeta_{sn}\phi_n + \zeta_{se}\phi_e + \zeta_{sr}Q_r, \tag{29}$$

$$Q_r = \zeta_{rs}Q_s + \zeta_{re}\phi_e. \tag{30}$$

To compute the transfer function $\phi_e(\mathbf{k}, \omega)/\phi_n(\mathbf{k}, \omega)$ we substitute (30) into (29) and isolate Q_s, giving

$$Q_s = \frac{\zeta_{sn}\phi_n + (\zeta_{se}+\zeta_{sre})\phi_e}{1-\zeta_{srs}}. \tag{31}$$

By substituting (31) in (28) and isolating Q_i we obtain

$$Q_i = \frac{\zeta_{ie}(1-\zeta_{srs}) + \zeta_{ise} + \zeta_{isre}}{(1-\zeta_{ii})(1-\zeta_{srs})}\phi_e + \frac{\zeta_{isn}}{(1-\zeta_{ii})(1-\zeta_{srs})}\phi_n. \tag{32}$$

Finally, by substituting (32) in (27) we obtain

$$(D-\zeta_{ee})\phi_e = \frac{\zeta_{esn}\phi_n + (\zeta_{ese}+\zeta_{esre})}{1-\zeta_{srs}}\phi_e + \frac{\zeta_{eie}(1-\zeta_{srs}) + \zeta_{eise} + \zeta_{eisre}}{(1-\zeta_{ii})(1-\zeta_{srs})}\phi_e \tag{33}$$

$$+ \frac{\zeta_{eisn}}{(1-\zeta_{ii})(1-\zeta_{srs})}\phi_n, \tag{34}$$

which can be rewritten as

$$\frac{\phi_e}{\phi_n} = \frac{\zeta_{eisn} + (1-\zeta_{ii})\zeta_{esn}}{[(D-\zeta_{ee})(1-\zeta_{srs})-\zeta_{ese}-\zeta_{esre}](1-\zeta_{ii})-\zeta_{eie}(1-\zeta_{srs})-\zeta_{eise}-\zeta_{eisre}}. \tag{35}$$

Appendix C. Steady-state firing rates

For an afferent input $\phi_n(x, t) = \phi_n$ that does not depend on time t and space x, the firing rates (Q_e, Q_i, Q_r, Q_s) might have spatially-homogeneous steady states (Q_e^*, Q_i^*, Q_r^*, Q_s^*). Equations for these can be derived as follows. By setting the spatial and temporal derivatives of the wave operator D to zero, it reduces to the unity operator, and hence (3) gives $\phi_e^* = Q_e^*$. Moreover, since the steady states (Q_e^*, Q_i^*, Q_r^*, Q_s^*) are independent of time t and space x they satisfy the following equations:

$$S^{-1}(Q_e^*) = h\otimes\nu_{ee}Q_e^* + h\otimes\nu_{es}Q_s^* + h\otimes\nu_{ei}Q_i^*, \tag{36}$$

$$S^{-1}(Q_i^*) = h\otimes\nu_{ie}Q_e^* + h\otimes\nu_{is}Q_s^* + h\otimes\nu_{ii}Q_i^*, \tag{37}$$

$$S^{-1}(Q_s^*) = h\otimes\nu_{sn}\phi_n + h\otimes\nu_{se}Q_e^* + h\otimes\nu_{sr}Q_r^*, \tag{38}$$

$$S^{-1}(Q_r^*) = h\otimes\nu_{rs}Q_s^* + h\otimes\nu_{re}Q_e^*, \tag{39}$$

where we have used that $Q_a^* = S(V_a^*)$, where V_a^* denotes the steady-state value of V_a for $a\in\{e, i, r, s\}$. Since the terms $\nu_{ab}Q_b^*$ do not depend on time, the convolutions $h\otimes\nu_{ab}Q_b^*$ reduce to

$$h\otimes\nu_{ab}Q_b^* = \nu_{ab}Q_b^*\int_0^\infty h(t)dt = \nu_{ab}Q_b^*\frac{H}{\eta}\int_0^\infty \bar{h}(t)dt = \nu_{ab}Q_b^*\frac{H}{\eta}, \tag{40}$$

which yields the steady-state equations

$$S^{-1}(Q_e^*) = \frac{H}{\eta}\nu_{ee}Q_e^* + \frac{H_c}{\eta_c}\nu_{ei}Q_i^* + \frac{H}{\eta}\nu_{es}Q_s^*, \tag{41}$$

$$S^{-1}(Q_i^*) = \frac{H}{\eta}\nu_{ie}Q_e^* + \frac{H_c}{\eta_c}\nu_{ii}Q_i^* + \frac{H}{\eta}\nu_{is}Q_s^*, \tag{42}$$

$$S^{-1}(Q_s^*) = \frac{H}{\eta}\nu_{sn}Q_n + \frac{H_c}{\eta_c}\nu_{se}Q_e^* + \frac{H_t}{\eta_t}\nu_{sr}Q_r^*, \tag{43}$$

$$S^{-1}(Q_r^*) = \frac{H}{\eta}\nu_{rs}Q_s^* + \frac{H_c}{\eta_c}\nu_{re}Q_e^*. \tag{44}$$

Note that the steady-states effectively depend on the *synaptic impacts* $\int_0^\infty \bar{h}(t)dt = H/\eta$ of the different types of receptors.

References

Adodra, S., Hales, T.G., 1995. Potentiation, activation and blockade of GABAA receptors of clonal murine hypothalamic GT1-7 neurones by propofol. Br. J. Pharmacol. 115 (6), 953–960 (July).

Alkire, M.T., Haier, R.J., Barker, S.J., Shah, N.K., Wu, J.C., Kao, Y.J., 1995. Cerebral metabolism during propofol anesthesia in humans studied with positron emission tomography. Anesthesiology 82, 393–403.

Alkire, M.T., Haier, R.J., Fallon, J.H., 2000. Toward a unified theory of narcosis: brain imaging evidence for a thalamocortical switch as the neurophysiologic basis of anesthetic-induced unconsciousness. Conscious. Cogn. 9 (3), 370–386 (September).

Alkire, M.T., Hudetz, A.G., Tononi, G., 2008. Consciousness and anesthesia. Science 322 (5903), 876.

Amari, S., 1977. Dynamics of pattern formation in lateral-inhibition type neural fields. Biol. Cybern. 27, 77–87.

Antkowiak, B., 1999. Different actions of general anesthetics on the firing patterns of neocortical neurons mediated by the GABAA receptor. Anesthesiology 500–511.

Bai, D., Pennefather, P.S., MacDonald, J.F., Orser, B.A., 1999. The general anesthetic propofol slows deactivation and desensitization of GABAA receptors. J. Neurosci. 19 (24), 10635 (December).

Bojak, I., Liley, D., 2005. Modeling the effects of anesthesia on the electroencephalogram. Phys. Rev. E 71 (4), 1–22 (April).

Breakspear, M., Roberts, J.A., Terry, J.R., Rodrigues, S., Mahant, N., Robinson, P.A., 2006. A unifying explanation of primary generalized seizures through nonlinear brain modeling and bifurcation analysis. Cereb. Cortex 16 (9), 1296–1313 (September).

Brown, E.N., Lydic, R., Schiff, N.D., 2010. General anesthesia, sleep, and coma. N. Engl. J. Med. 363 (27), 2638–2650.

Ching, S., Cimenser, A., Purdon, P.L., Brown, E.N., Kopell, N.J., 2010. Thalamocortical model for a propofol-induced {alpha}-rhythm associated with loss of consciousness. Proc. Natl. Acad. Sci. U. S. A. 107, 22665–22670 (December).

Cimenser, A., Purdon, P.L., Pierce, E.T., Walsh, J.L., Salazar-Gomez, A.F., Harrell, P.G., Tavares-Stoeckel, C., Habeeb, K., Brown, E.N., 2011. Tracking brain states under general anesthesia by using global coherence analysis. Proc. Natl. Acad. Sci. U. S. A. 108 (21), 8832–8837 (May).

Daunizeau, J., David, O., Stephan, K.E., 2009. Dynamic causal modelling: a critical review of the biophysical and statistical foundations. NeuroImage 1–11 (December).

David, O., Harrison, L., Friston, K.J., 2005. Modelling event-related responses in the brain. NeuroImage 25 (3), 756–770 (April).

Deco, G., Jirsa, V.K., Robinson, P.A., Breakspear, M., Friston, K., 2008. The dynamic brain: from spiking neurons to neural masses and cortical fields. PLoS Comput. Biol. 4 (8), e1000092 (January).

Doyle, P.W., Matta, B.F., 1999. Burst suppression or isoelectric encephalogram for cerebral protection: evidence from metabolic suppression studies. Br. J. Anaesth. 83 (4), 580–584 (October).

Feshchenko, V.A., Veselis, R.A., Reinsel, R.A., 2004. Propofol-induced alpha rhythm. Neuropsychobiology 50 (3), 257–266 (January).

Fiset, P., Paus, T., Daloze, T., Plourde, G., Meuret, P., Bonhomme, V., Hajj-Ali, N., Backman, S.B., Evans, A.C., 1999. Brain mechanisms of propofol-induced loss of consciousness in humans: a positron emission tomographic study. J. Neurosci. 19 (13), 5506–5513 (July).

Foster, B.L., Bojak, I., Liley, D.T.J., 2008. Population based models of cortical drug response: insights from anaesthesia. Cogn. Neurodyn. 2 (4), 283–296 (December).

Freeman, W.J., 2004. Mass action in the nervous system.

Gugino, L.D., Chabot, R.J., Prichep, L.S., John, E.R., Formanek, V., 2001. Quantitative EEG changes associated with loss and return of consciousness in healthy adult volunteers anaesthetized with propofol or sevo Â¯ urane. Br. J. Anaesth. 87 (3), 421–428.

Hazeaux, C., Tisserant, D., Vespignani, H., Hummer-Sigiel, L., Kwan-Ning, V., Laxenaire, M.C., 1987. Electroencephalographic changes produced by propofol. Ann. Fr. Anesth. Reanim. 6, 261–266.

Hemmings, H.C., Akabas, M.H., Goldstein, P.A., Trudell, J.R., Orser, B.A., Harrison, N.L., 2005. Emerging molecular mechanisms of general anesthetic action. Trends Pharmacol. Sci. 26 (10), 503–510 (October).

Hindriks, R., Bijma, F., van Dijk, B.W., Stam, C.J., van der Werf, Y.Y., van Someren, E.J.W., de Munck, J.C., van der Vaart, A.W., 2011. Data-driven modeling of phase interactions between spontaneous MEG oscillations. Hum. Brain Mapp. (000:n/a–n/a, January).

Huotari, A.M., 2004. Evoked EEG patterns during burst suppression with propofol. Br. J. Anaesth. 92 (1), 18–24 (January).

Hutt, A., Longtin, A., 2010. Effects of the anesthetic agent propofol on neural populations. Cogn. Neurodyn. 4, 37–59 (September).

Jansen, B.H., Rit, V.G., 1995. Electroencephalogram and visual evoked potential generation in a mathematical model of coupled cortical columns. Biol. Cybern. 366, 357–366.

Jirsa, V.k., Haken, H., 1996. Field theory of electromagnetic brain activity. Phys. Rev. Lett. 77 (5), 960–963 (July).

Johnson, B.W., Sleigh, J.W., Kirk, I.J., Williams, M.L., 2003. High-density EEG mapping during general anaesthesia with xenon and propofol: A pilot study. Anaesth. Intensive Care 31 (2), 155–163.

Jurd, R., Arras, M., Lambert, S., Drexler, B., 2003. General anesthetic actions in vivo strongly attenuated by a point mutation in the GABA A receptor. FASEB J. 250–252.

Kandel, E.R., Schwartz, J.H., Jessell, T.M., 2000. Principles of neuroscience.

Kitamura, A., Marszalec, W., Yeh, J.Z., Narahashi, T., 2003. Effects of halothane and propofol on excitatory and inhibitory synaptic transmission in rat cortical neurons. J. Pharmacol. Exp. Ther. 304 (1), 162–171.

Krasowski, M.D., Koltchine, V.V., Rick, C.E., Ye, Q., Finn, S.E., Harrison, N.L., 1998. Propofol and other intravenous anesthetics have sites of action on the gamma-aminobutyric acid type A receptor distinct from that for isoflurane. Mol. Pharmacol. 53 (3), 530–538 (March).

Kuizenga, K., Wierda, J.M.K.H., Kalkman, C.J., 2001. Biphasic EEG changes in relation to loss of consciousness during induction with thiopental, propofol, etomidate, midazolam or sevoflurane. Br. J. Anaesth. 86 (3), 354–360.

Liley, D.T.J., Bojak, I., 2005. Understanding the transition to seizure by modeling the epileptiform activity of general anesthetic agents. J. Clin. Neurophysiol. 22 (5), 300–313 (October).

Liley, D.T.J., Cadusch, P.J., 2002. A spatially continuous mean field theory of electrocortical activity. Network: Comput. Neural Syst. 13 (1), 67–113 (February).

Liley, D., Cadusch, P., Gray, M., Nathan, P., 2003. Drug-induced modification of the system properties associated with spontaneous human electroencephalographic activity. Phys. Rev. E 68 (5), 1–15 (November).

Lopes da Silva, F.H., Hoeks, A., Smits, H., Zetterberg, L.H., 1974. Model of brain rhythmic activity. Kybernetic 15, 27–37.

Loxley, P.N., Robinson, P.A., 2007. Spike-rate adaptation and neuronal bursting in a mean-field model of brain activity. Biol. Cybern. 97 (2), 113–122 (August).

Lukatch, H.S., Kiddoo, C.E., Maciver, M.B., 2005. Anesthetic-induced burst suppression EEG activity requires glutamate-mediated excitatory synaptic transmission. Cereb. Cortex 15 (9), 1322–1331 (September).

McCarthy, M.M., Brown, E.N., Kopell, N., 2008. Potential network mechanisms mediating electroencephalographic beta rhythm changes during propofol-induced paradoxical excitation. J. Neurosci. 28 (50), 13488–13504 (December).

McKernan, R.M., 1996. Which GABAA-receptor subtypes really occur in the brain? Trends Neurosci. 19 (4), 139–143.
Mhuircheartaigh, R.N., Rosenorn-Lanng, D., Wise, R., Jbabdi, S., Rogers, R., Tracey, I., 2010. Cortical and subcortical connectivity changes during decreasing levels of consciousness in humans: a functional magnetic resonance imaging study using propofol. J. Neurosci. 30 (27), 9095–9102 (July).
Molaee-Ardekani, B., Senhadji, L., Shamsollahi, M., Vosoughi-Vahdat, B., Wodey, E., 2007. Brain activity modeling in general anesthesia: enhancing local mean-field models using a slow adaptive firing rate. Phys. Rev. E 76 (4), 1–17 (October).
Nunez, P.L., Srinivasan, R., 2006. Electric fields of the brain. The neurophysics of EEG.
Rennie, C.J., Robinson, P.A., Wright, J.J., 2002. Unified neurophysical model of EEG spectra and evoked potentials. Biol. Cybern. 86 (6), 457–471 (June).
Robinson, P.A., Rennie, C.J., Wright, J.J., 1997. Propagation and stability of waves of electrical activity in the cerebral cortex. Phys. Rev. E 56 (1), 826 (July).
Robinson, P., Rennie, C., Wright, J., Bahramali, H., Gordon, E., Rowe, D., 2001. Prediction of electroencephalographic spectra from neurophysiology. Phys. Rev. E 63 (2), 19–33 (January).
Robinson, P., Rennie, C., Rowe, D., 2002. Dynamics of large-scale brain activity in normal arousal states and epileptic seizures. Phys. Rev. E 65 (4), 1–9 (April).
Rowe, D.L., Robinson, P.A., Rennie, C.J., 2004. Estimation of neurophysiological parameters from the waking EEG using a biophysical model of brain dynamics. J. Theor. Biol. 231 (3), 413–433 (December).
Rudolph, U., Antkowiak, B., 2004. Molecular and neuronal substrates for general anaesthetics. Nat. Rev. Neurosci. 5 (9), 709–720 (September).
San-juan, D., Chiappa, K.H., Cole, A.J., 2010. Propofol and the electroencephalogram. Clin. Neurophysiol. 121 (7), 998–1006 (July).
Schwender, D., Daunderer, M., Mulzer, S., Klasing, S., Finsterer, U., Peter, K., 1996. Spectral edge frequency of the electroencephalogram to monitor "depth" of anaesthesia with isoflurane or propofol. Br. J. Anaesth. 77 (2), 179 (August).
Sieghart, W., Sperk, G., 2002. Subunit composition, distribution and function of GABA_A receptor subtypes. Curr. Top. Med. Chem.
Stam, C.J., Pijn, J.P.M., Suffczynski, P., Lopes da Silva, F.H., 1999. Dynamics of the human alpha rhythm: evidence for non-linearity? Clin. Neurophysiol. 110 (10), 1801–1813 (October).
Steyn-Ross, M.L., Steyn-Ross, D.A., Sleigh, J.W., Liley, D.T., 1999. Theoretical electroencephalogram stationary spectrum for a white-noise-driven cortex: evidence for a general anesthetic-induced phase transition. Phys. Rev. E Stat. Phys. Plasmas Fluids Relat. Interdiscip. Topics 60 (6 Pt B), 7299–7311 (December).
Steyn-Ross, D.A., Steyn-Ross, M.L., Sleigh, J.W., Wilson, M.T., Gillies, I.P., Wright, J.J., 2005. The sleep cycle modelled as a cortical phase transition. J. Biol. Phys. 31 (3–4), 547–569 (December).
van Putten, M.J.A.M., Peters, J.M., Mulder, S.M., de Haas, J.M., Bruijninckx, C.M.A., Tavy, D.L.J., 2004. A brain symmetry index (BSI) for online EEG monitoring in carotid endarterectomy. Clin. Neurophysiol. 115 (5), 1189–1194 (May).
Velly, L.J., Rey, M.F., Bruder, N.J., Gouvitsos, F.A., Witjas, T., Regis, J.M., Peragut, J.C., Gouin, F.M., 2007. Differential dynamic of action on cortical and subcortical structures of anesthetic agents during induction of anesthesia. Anesthesiology 107 (2), 202 (August).
White, N.S., Alkire, M.T., 2003. Impaired thalamocortical connectivity in humans during general-anesthetic-induced unconsciousness. NeuroImage 19 (2), 402–411 (June).
Whittington, M.A., Jefferys, J.G., 1996. Effects of intravenous anaesthetic agents on fast inhibitory oscillations in the rat hippocampus in vitro. Br. J. Pharmacol. 118 (8), 1977–1986 (August).
Wilson, H.R., Cowan, J.D., 1973. A mathematical theory of the functional dynamics of cortical and thalamic nervous tissue. Kybernetik 13 (2), 55–80 (September).
Xiang, Z., Huguenard, J.R., Prince, D.A., 1998. GABAA receptor-mediated currents in interneurons and pyramidal cells of rat visual cortex. J. Physiol. 506 (3), 715–730 (February).